MULTISPECTRAL REMOTE SENSING ALGORITHMS FOR PARTICULATE ORGANIC CARBON (POC) AND ITS TEMPORAL AND SPATIAL VARIATION

Young Baek Son[1]; Meng Hua Wang[1]; Wilford D. Gardner[2]
[1] National Oceanographic and Atmospheric Administration, 5200 Auth Rd., Camp Spring, MD 20852 USA, youngbaek.son@noaa.gov; menghua.wang@noaa.gov
[2] Dep. of Oceanography, Texas A&M Univ., College Station, TX 77843 USA, wgarder@ocean.tamu.edu

ABSTRACT

Hydrographic data including particulate organic carbon (POC) from the Northeastern Gulf of Mexico (NEGOM) study were used along with remotely sensed data obtained from NASA's Sea-viewing Wide Field-of-view Sensor (SeaWiFS) to develop POC algorithms to estimate POC concentration based on empirical and model-based principal component analysis (PCA) methods. In Case I and II waters empirical maximized simple ratio (MSR) and model-based PCA algorithms using full wavebands (blue, green and red wavelengths) provide more robust estimates of POC. The predicted POC concentrations matched well the spatial and seasonal distributions of POC measured *in situ* in the Gulf of Mexico. The ease in calculating the MSR algorithm compared to PCA analysis makes MSR the preferred algorithm for routine use.

In order to determine the inter-annual variations of POC, MSR algorithms applied to calculate 100 monthly mean values of POC concentrations (September 1997-December 2005). The spatial and temporal variations of POC and sea surface temperature (SST) were analyzed with the empirical orthogonal function (EOF) method. POC estimates showed inter-annual variation in three different locations and may be affected by El Niño/Southern Oscillation (ENSO) events.

KEY WORDS: Ocean Color, Particulate Organic Carbon (POC), SeaWiFS, EOF, ENSO event

INTRODUCTION

As we strive to better understand carbon cycling in the ocean, it is important to be able to measure particulate organic carbon (POC) as well as dissolved organic and inorganic constituents effectively. POC generally may be a small component of the total carbon, but since POC can sink through the water column, it plays an important role in sequestering carbon as part of the biological pump. Studies such as the Joint Global Ocean Flux Study (JGOFS), World Ocean Circulation Experiment (WOCE), and South Atlantic Ventilation Experiment (SAVE) have greatly expanded our knowledge on many parameters of the carbon pool as well as hydrography. Estimates of surface POC concentration using SeaWiFS products and *in situ* POC measurements have also been made (Stramski et al., 1999; Loisel et al., 2001; Mishonov et al., 2003; Stramska and Stramski, 2005; Gardner et al., 2006) and provide reasonable assessment of POC distribution on regional to global scales. Some of these approaches used single wavelengths instead of multiple spectral bands, but a single wavelength method cannot account for the non-linear response in optically complex environments. For further progress we need to employ an empirical and model-based approaches based on spectral remote sensing data for more accurate POC estimates. It is important for quantifying the time-varying evolution of POC in surface waters to monitors, and eventually model, the impact of climate change.

The purpose of this study is to develop accurate and efficient POC algorithms based on satellite products; to compare POC estimates with *in situ* measurements; to investigate the advantages and disadvantages of various POC algorithms; and to determine inter-annual variation in temporal and spatial POC estimates based on ocean color data and physical processes.

DATA AND METHODS

During the NEGOM project, data from approximately 100 CTD/transmissometer/fluorometer casts were collected on each of nine seasonal cruises from November 1997 to August 2000 along the same eleven track lines normal to the coastline between mid-Florida and the Mississippi River, starting from about 20m water depth on the shelf and moving out to the 1,000m isobath (Figure 1).

To estimate POC concentration, we compared shipboard data with satellite-derived ocean color data obtained synchronously. Data from SeaWiFS ocean color data from November 1997 to August 2000 were obtained from the NASA Goddard Space Flight Center DAAC (http://oceancolor.gsfc.nasa.gov/) and were generated using SeaWiFS Data Analysis System (SeaDAS) program. For comparing SeaWiFS and *in-situ* data, values were extracted from 3×3 pixels box at each NEGOM station location and averaged (Figure 1). The

data were used to estimate the POC concentration using an empirical (Son et al., submitted) and principal component analysis (PCA) (Son, 2006).

In order to detect temporal and spatial patterns of a large ocean color data set, empirical orthogonal function (EOF) analysis was calculated with a monthly time-series data of POC estimates and sea surface temperature (SST) data during 100 months (September 1997 to December 2005).

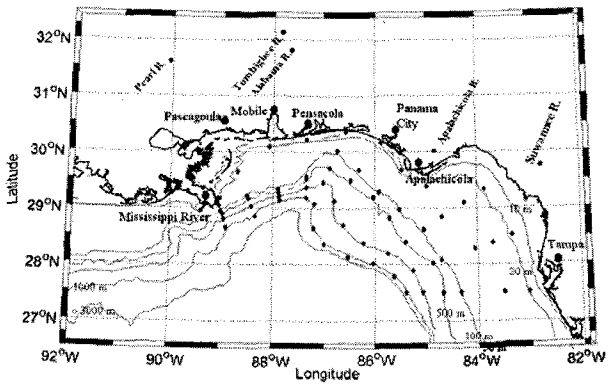

Figure 1. Bathymetry and sampling stations in the Northeastern Gulf of Mexico (NEGOM) (11 sampling transects with 60 POC sampling stations each).

RESULTS

Seasonal Patterns of POC

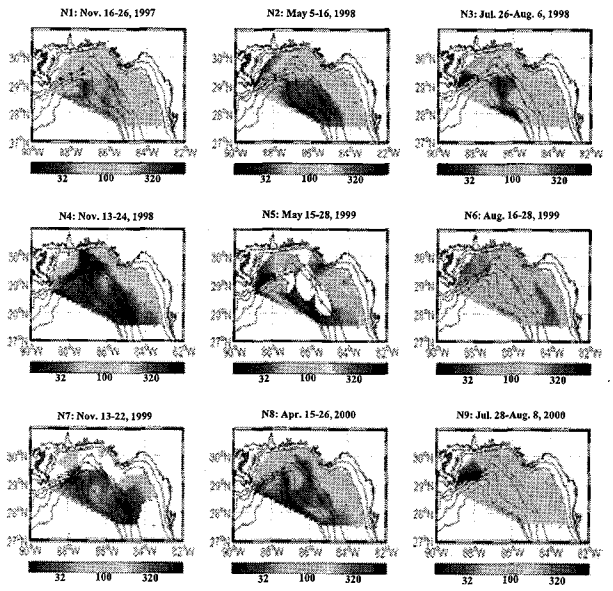

Figure 2. Surface particulate organic carbon concentration ($mg \cdot m^{-3}$) contoured from bottle samples collected at ~60 stations during each NEGOM hydrographic cruise.

During the fall cruises (1997 - N1, 1998 - N4, and 1999 - N7), higher POC concentrations were generally confined to the inner shelf. These concentrations decreased across the outer shelf and the upper slope (Figure 2). During the spring cruises (1998 - N2, 1999 - N5, and 2000 - N8), most high POC concentrations occurred between Mobile Bay and the Mississippi delta, the area which receives high inputs from the Mississippi, Pearl, and Tombigbee (Alabama) river (Figure 1 and 2).

Spatial distribution of POC concentration was significantly different during summer seasons (1998 - N3, 1999 - N6, and 2000 - N9, Figure 2). Elevated surface POC concentrations (> 300 mg·m-3) extended over the upper slope across the study area. A wide swath of higher than expected POC concentration was located across the midsection of the region in a northwest-southeast direction.

Empirical Approaches

In this study, measurements of the spectral radiance upwelled from the ocean were used to estimate POC concentration. The analysis was applied to spectral radiance acquired at every POC station for the full SeaWiFS spectral range of 410-670 nm, using 6 wavelengths (Figure 3). When the POC concentration in the surface water increased, the radiance peak shifted from the shorter wavelength (412 and 443 nm, violet-blue) to longer wavelengths (555 nm, green) because radiance from particles dominates the signal. Radiance at 510 nm remained relatively constant over a wide range of POC concentrations (< 20 to > 550 $mg \cdot m^{-3}$).

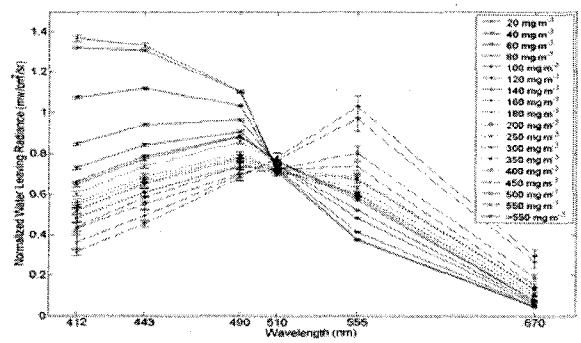

Figure 3. Normalized water-leaving radiance *versus* SeaWiFS wavelengths averaged over areas with different binned POC concentrations (1-750 $mg \cdot m^{-3}$).

In the first approach we calculated a regression between POC and chlorophyll concentrations using a linear curve estimate that showed a fairly constant relationship (R = 0.89, Eq.1 in Table 1). Low POC concentrations have a close relationship with low chlorophyll values, but the correlation is not as tight at higher POC and chlorophyll concentrations. The regression between POC and K_{490} was moderate (R=0.88, Eq.2 in Table 1), but it was less sensitive at higher POC concentrations, where scatter also increases.

In the second approach using single wavelength algorithms at 555 nm, *Lwn* or *Rrs* were well correlated at low concentrations but scatter increased at higher POC concentrations (R = 0.86, Eq.3 in Table 1). Lower POC concentrations were well correlated with 555 nm using algorithms of both Stramski et al. (1999) and Mishonov et al. (2003), but at higher POC those algorithms have a

lower correlation because they were developed with data from open ocean where living as well as nonliving organic terrigenous particles are less abundant.

In our third approach we tested several *Rrs* and *Lwn* green-to-red/green wavelength ratios (555/510 and 670/510, or 510/555 and 670/555) for correlations with POC. Radiance at 510 and 555 nm were used as normalizing factors because at those wavelengths there is relatively minor variability in spectral absorption due to particulate and dissolved substances. The green-to-red/green ratio provided a statistically better estimate of POC concentration (R=0.89, Eq.4 in Table 1) than the blue-to-green ratio.

In our fourth approach a simple ratio (SR) was used to determine the relationship using one green and one blue wavelength and POC. SR values are directly (but not linearly) proportional to POC concentrations (R=0.86, Eq.5 in Table 1).

A fifth approach, the maximized simple ratio (MSR), was based on the same concepts as the SR, but used all blue-to-green wavelengths. To reduce the scatter of the radiance signal, we used the 510 nm value as a normalizing factor. In the shorter wavelengths, the maximum radiance value among 412, 443, and 490 nm was normalized by the value at 510 nm. In the green wavelengths, peaks were consistently at 555 nm, so the ratios using 555 nm to 510 nm were evaluated. MSR values were directly (but not linearly) proportional to POC concentrations. This method produced better results than the first four approaches, especially when predicting high POC concentrations (R=0.91, Eq.6 in Table 1).

Model-Based Approach (PCA)

The total variance (eigenvalue) calculated by the PCA method. The first five modes accounted for 99.94% of total variance. In examining individual eigenvectors, the first eigenvector showed a peak at the shortest wavelength measured – 412 nm. The peak in the second eigenvector occurred at 555 nm, and the third eigenvector peak was at 490 nm. The rest of the eigenvectors had double peaks.

A least-squares fit of the principal component (PC) values to POC concentrations using the multiple-linear regression method showed that POC estimates ($mg \cdot m^{-3}$) were related to each principal component of the SeaWiFS visible wavelengths (R=0.92, Eq.7 in Table 1). The first three vectors demonstrate different weighting factors with varying POC concentration. One, or a combination, of the weighted eigenvalues reduced the noise levels from an optically complex environment (Son, 2006).

POC Estimates in Case I and II Waters

The correlation between *in situ* POC and POC estimates obtained from different algorithms evaluated in this study is displayed in Figure 4. POC concentration was under-estimated when based on SeaWiFS chlorophyll pigment concentration (Eq. 1) and over-estimated when based on SeaWiFS K_{490} (Eq. 2). The single-wavelength radiance (or remote-sensing reflectance) algorithm using 555 nm over-estimated low, and under-estimated high POC concentrations (Eq. 3). The simple ratio (Eq. 5) under-estimated high POC concentrations compared to regressions based on chlorophyll (Eq. 1) or green-to-red/green ratio algorithms (Eq. 4). The MSR and PCA algorithms produced a very good correlation between *in situ* POC and derived POC values at all concentrations (Eq. 6 and Eq. 7).

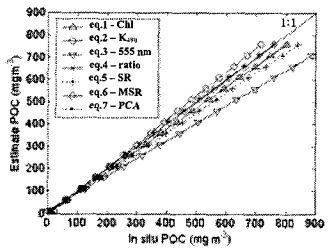

Figure 4. Comparison of *in situ* POC and predicted POC concentration obtained using seven different approaches. MSR and PCA approaches (eq.6 and eq.7) employ full spectral radiance information and are well correlated with a broad range of POC concentrations, providing better estimates than single wavelength or simple blue-to-green ratio approaches.

Table 1. Least-squares fit of regression between POC and SeaWiFS products.

Equation ($mg \cdot m^{-3}$)	R	RMSE
(1) $POC = 10^{(0.70144 \times \log(chl) + 2.05478)}$	0.89	0.182
(2) $POC = 10^{(2.047 \times \log(K_{490}) + 3.835)}$	0.88	0.182
(3) $POC = 10^{(2.16 \times \log(Rrs(555)) + 7.412)}$ or $POC = 10^{(2.155 \times \log(Lwn(555)) + 2.505)}$	0.86	0.205
(4) $POC = 10^{(2.964 \times R_{54} - 0.14 \times R_{64} + 2.174)}$ or $POC = 10^{(2.945 \times L_{54} - 0.14 \times L_{64} + 2.205)}$ or $POC = 10^{(-2.823 \times R_{45} - 0.14 \times R_{65} + 2.174)}$ or $POC = 10^{(-2.808 \times L_{45} - 0.14 \times L_{65} + 2.205)}$	0.89	0.182
(5) $POC = 141.30e^{(SRRrs \times 2.63)}$ or $POC = 142.29e^{(SRLwn \times 2.62)}$	0.86	0.189
(6) $POC = 700.20 \times MSRRrs^3 + 1289.89 \times MSRRrs^2 + 839.98 \times MSRRrs + 226.61$ or $POC = 675.73 \times MSRLwn^3 + 1288.37 \times MSRLwn^2 + 864.15 \times MSRLwn + 235.07$	0.91	0.181
(7) $POC = -111.1 \times PC_1 + 342.2 \times PC_2 - 535.1 \times PC_3 + 737.2 \times PC_4 - 770.9 \times PC_5 + 98.1$	0.92	0.178

(chl is the chlorophyll concentration derived from the current SeaWiFS chlorophyll algorithm (OC4v4), k490 is diffuse attenuation coefficient at 490 nm, R_{ij} (or L_{ij}) is the log-transformed ratio of $Rrs(\lambda_i)$ to $Rrs(\lambda_j)$ ($Lwn(\lambda_i)$ to $Lwn(\lambda_j)$) and the subscripts i and j are wavelengths (1-6) that represented SeaWiFS wavebands 412(1), 443(2), 490(3), 510(4), 555(5), and 670(6) nm, SRRrs (SRLwn) is [(Rrs(555)-Rrs(443))/(Rrs(555)+Rrs(443))] or ([(Lwn(555)-Lwn(443))/(Lwn(555)+ Lwn(443))]), MSRRrs (MSRLwn) is [{Rrs(555)/Rrs(510)-(Rrs(412)>Rrs(443)>Rrs(490))/Rrs(510)}/[{Rrs(555)/Rrs(510)+(Rrs(412)>Rrs(443)>Rrs(490))/Rrs(510)}] or [{Lwn(555)/ Lwn(510)-(Lwn(412)>Lwn(443)>Lwn(490))/Lwn(510)}/[{Lwn(555)/Lwn(510)+(Lwn(412)>Lwn(443)>Lwn(490))/Lwn(510)}], and $PC_{1,2,....5}$ are the PC of the first, second, ..., and fifth mode).

Spatial and Temporal Variations of POC using EOF Analysis

Each EOF unit was interpreted considering amplitude and spatial patterns as unit of information. A given EOF pattern described a spatial pattern of residual variance, which was modulated by its corresponding time-varying amplitude. This provided spatial and

temporal patterns and elucidated the relationship between POC concentration and physical processes.

In Figure 5, the spatial SST and POC patterns in the first modes revealed important climatic variability on inter-annual timescale. The non-seasonal time-series indicated that POC concentration was strongly affected by the enhancement of large-scale processes. The low frequency SST signal in Equatorial Pacific Ocean (Figure 5 e-f) showed El Niño/Southern Oscillation (ENSO), which is the most important coupled ocean-atmosphere phenomenon to cause global climate variability on interannual time scales. Variability between SST and POC in Pacific Ocean are temporally and spatially correlated with large-scale fluctuations and similar to different locations (Korea and the Gulf of Mexico). These remote effects of El Niño are referred to as teleconnections (McPhaden, 2002). During El Nino events (1997-1998 and 2002-2004) POC showed relatively positive amplitudes and relatively negative values during La Niña conditions (1999-2001). Time series of POC and SST in Korea and the Gulf of Mexico had 3-6 month lag times from ENSO signal. Temporal and spatial surface POC concentrations may be strongly affected by interannually varying the forces likely to govern climate variability.

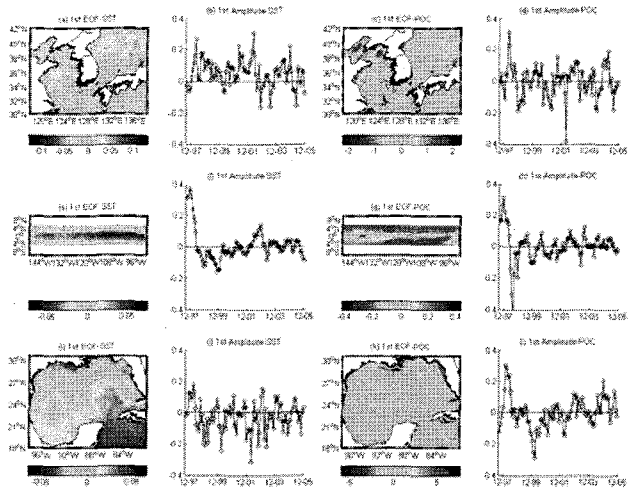

Figure 5. First temporal mode of SST and POC for EOF patterns and its time series in Korea (a-d), Nino3 region (e-h), and the Gulf of Mexico (i-l).

CONCLUSIONS

The classical approach for estimating upper ocean parameters using remote sensing data is to develop empirical and model-based algorithms. Using a large data set that included *in situ* measurements and satellite-derived ocean color products, we tested simple empirical and model-based approaches to derive POC concentration.

Our analysis of the spectral response demonstrated that the radiance was significantly dependent on POC concentration or other water constituents, and that the radiance peak shifted significantly from violet-blue wavelength to green wavelength as POC concentration increased. Based on this spectral dependence, several approaches, including radiance ratios of different wavelengths, were pursued to better estimate POC concentrations. The approaches using multiple wavelength radiances were more sensitive to these non-linear conditions than using single wavelength radiance or blue-to-green ratios, and provided reliable estimates over a wide range of surface POC concentrations. In this study, the best estimates for POC concentrations were achieved with MSR algorithm.

To understand temporal and spatial relationships between POC and impact of climate change, 100-month satellite estimates of POC and SST were investigated. These inter-annual differences of POC concentrations over the study period were affected by one or more physical factors related to ocean-atmospheric forcing such as ENSO events.

REFERENCES

Gardner, W.D., A.V. Mishonov, and M.J. Richardson, 2006. Global POC concentrations from in-situ and satellite data, *Deep Sea Res., Part II,* 53, pp.718-740.

Loisel, H., and A. Morel, 1998. Light scattering and chlorophyll concentration in case 1 water: a reexamination, *Limnol. Oceanogr., 43*, pp. 847-858.

McPhaden, M.J., 2002. El Niño and La Niña: Causes and Global Consequences. In: *Encyclopedia of Global Environmental Change, Vol 1*, John Wiley and Sons, Ltd., Chicester, UK, pp. 353-370.

Mishonov, A.V., W.D. Gardner, and M.J. Richardson, 2003. Remote sensing and surface POC concentration in the South Atlantic, *Deep Sea Res., Part II, 50*, pp. 2997-3015.

Son, Y.B., 2006. POC algorithms based on spectral remote sensing data and its temporal and spatial variability in the Gulf of Mexico, Ph.D. thesis, 200 pp., Texas A&M Univ., College Station.

Son, Y.B., W.D. Gardner, A.V. Mishonov, and M.J. Richardson, Multispectral remote sensing algorithms for particulate organic carbon (POC), *J. Geophys. Res.*, submitted.

Stramska, M., and D. Stramski, 2005. Variability of particulate organic carbon concentration in the north polar Atlantic based on ocean color observation with Sea-viewing Wide Field-of-view Sensor (SeaWiFS), *J. Geophys. Res.*, 110, C10018, doi:10.1029/2004JC002762.

Stramski, D., R.A. Reynolds, M. Kahru, and B.G. Mitchell, 1999. Estimation of particulate organic carbon in the ocean from satellite remote sensing, *Science, 285*, pp. 239-242.

ACKNOWLEDGEMENTS

This research was performed while the author held a National Research Council Research Associateship Award at NOAA.